

# Formation Process of Taylor-Görtler Vortex

H. Yamaguchi Ph. D

## Abstract

Formation process of Taylor-Görtler vortex in the gap between two concentric spheres is investigated numerically. The axisymmetric Navier-Stokes equations are solved for the laminar viscous flow with the stationary outer sphere and the rotating inner sphere. The results obtained show qualitative agreement with the experiments reported by Wimmer and Nakabayashi. The numerical results obtained in the present study indicates that prior to the formation of Taylor-Görtler vortex, a very weak independent vortex appears in the boundary layer formed on the inner sphere. The boundary layer then separated at the region where the weak vortex appears, and on the next instant the cellular structure of vortices occupies the gap space as Taylor-Görtler vortices.

## Introduction

The motion of the fluid contained between two concentric spheres in rotating systems has received much attention over the past decade, particularly in the field of geophysics and engineering design.

Taylor (1) investigated the fluid motion between two concentric rotating cylinders with inner one rotating and the outer one stationary. When the rotational velocity is very small, the flow becomes a simple shear flow, which is the basic flow (Couette flow), in the direction of the rotation. By increasing the rotational velocity and at a critical Reynolds number, the hydrodynamic instability causes the flow to form a cellular pattern structure of vortices in the gap space.

Similar phenomena appears for the flow between two concentric rotating spheres with a common axis. However, in the case of spheres the centrifugal forces are a function of the latitude, resulting in the existence of different types of flow pattern. Theoretical and experimental works have been carried out by many researchers. Wimmer (2) and Nakabayashi (3) conducted their experiments and reported various phenomena of flow regarding the formation of Taylor-Görtler vortices in sufficient details. On the other hand, theoretical works have been done by Munson et al (4) (with experimental studies as well) and Schrauf (5). The works

The circumferential components of the equations (2), (g) and (3) are now shown as:

$$\frac{\delta \Omega}{\delta t} + v_r \frac{\delta \Omega}{\delta r} + \frac{v_\theta}{r} \frac{\delta \Omega}{\delta \theta} = \nu D^2 \Omega \quad (9)$$

$$\frac{\delta \zeta}{\delta t} + v_r \frac{\delta \zeta}{\delta r} + \frac{v_\theta}{r} \frac{\delta \zeta}{\delta \theta} + \frac{2 \Omega}{r^3 \sin \theta}$$

$$\left( \frac{\delta \Omega}{\delta \theta} - \frac{\delta \Omega}{\delta r} r \cot \theta \right) - \frac{2 \zeta}{r} (v_r + v_\theta \cot \theta)$$

$$= \nu D^2 \zeta \quad (10)$$

$$D^2 \psi = \zeta \quad (11)$$

where  $D^2$  is a differential operator defined as:

$$D^2 = \frac{\delta^2}{\delta r^2} + \frac{1}{r^2} \frac{\delta^2}{\delta \theta^2} - \frac{\cot \theta}{r^2} \frac{\delta}{\delta \theta} \quad (12)$$

The vorticity used in the equation (9), (10) is a direction component of vorticity vector.

$$\zeta = \bar{\zeta} \cdot \hat{\phi} \quad (13)$$

In order to nondimensionalize the equations (9) (10) and (11), the following parameters are introduced.

$$\text{Stream function : } S = \frac{\psi}{\omega_o r_2^3}$$

$$\text{Angular velocity : } F = \frac{\Omega}{\omega_o r_2^2}$$

$$\text{Radius : } R = \frac{r_1}{r_2}$$

$$\text{Angular velocity : } \omega_1 = \frac{\omega_1^*}{\omega_o}$$

$$\text{Vorticity : } V = \frac{\zeta}{\omega_o r_2}$$

$$\text{Reynolds No. : } Re = \frac{\omega_o r_2^2}{\nu}$$

$$\text{Velocity : } (u, v, w) = \frac{(v_r, v_\theta, v_\phi)}{\omega_o r_2}$$

$$\text{Gap ratio : } \sigma = \frac{r_2 - r_1}{r_2} = 1 - \gamma \quad (14)$$

where  $\omega_o$  is a reference angular velocity. It is noted that the suffix 1 and 2 indicate the inner and outer spheres respectively. The following sets of nondimensional equations are then reduced :

$$u = \frac{1}{R^2 \sin \theta} \frac{\delta S}{\delta \theta}, \quad v = -\frac{1}{R \sin \theta} \frac{\delta S}{\delta R}, \quad w = \frac{F}{R \sin \theta} \quad (15)$$

$$\frac{\delta F}{\delta t} + u \frac{\delta F}{\delta R} + \frac{v}{R} \frac{\delta F}{\delta \theta} = \frac{1}{Re} D^2 F \quad (16)$$

$$\frac{\delta V}{\delta t} + u \frac{\delta V}{\delta R} + \frac{v}{R} \frac{\delta V}{\delta \theta} + \frac{2 F}{R^3 \sin \theta} \left( \frac{\delta F}{\delta \theta} - \frac{\delta F}{\delta R} R \cot \theta \right) - \frac{2 V}{R} (u + v \cot \theta) = \frac{1}{Re} D^2 V \quad (17)$$

$$D^2 S = V \quad (18)$$

$$\text{where } D^2 = \frac{\delta^2}{\delta R^2} + \frac{1}{R^2} \frac{\delta^2}{\delta \theta^2} - \frac{\cot \theta}{R^2} \frac{\delta}{\delta \theta} \quad (19)$$

### Boundary Conditions

The boundary conditions are Stokes' no-slip condition at the walls of the spheres, while at the equatorial plane  $\theta = \pi/2$  and the axis of rotation  $\theta = 0$ , the symmetric conditions are imposed. The vorticity on two walls is solved with the condition of  $\delta S / \delta R = 0$ . Fig. 2 shows a schematic diagram of the boundary conditions. The inner sphere rotates with an arbitrary angular velocity  $\omega_1^*(t)$  and the outer sphere is kept stationary. The angular acceleration of the inner sphere in the spin-up period is defined as  $\frac{d\omega_1^*}{dt} = \text{const}$ . The constant is determined from a given steady angular velocity and the time step chosen in the calculation.



deal with the instability of the fluid to estimate the critical Reynolds number as well as predicting the field. Among others, there are papers by Pearson (6) and Bartels (7) who solved the governing partial differential equations with the finite difference method. Various modes of the flow were investigated with different conditions. However, since their results are shown for time infinity in which the flow reaches the steady state, no detailed process of forming Taylor-Görtler vortex has been found.

In this study, time dependent formation process of the Taylor-Görtler vortex is concerned for the flow field in spherical gaps where Taylor-Görtler vortices are expected. In order to obtain a typical case, spacial and physical parameters are chosen according to the Wimmer's (2) experiments. The unsteady motion of an incompressible viscous fluid is considered when the inner sphere is impulsively accelerated to a given angular velocity. Axisymmetric Navier-Stokes equations written in terms of the stream function, angular velocity function and the vorticity are solved by means of the finite difference technique for the initially stationary flow.

### Basic Equations.

Incompressible viscous hydrodynamic equations are:

$$\nabla \cdot \mathbf{v} = 0 \quad (1)$$

$$\frac{D\mathbf{v}}{Dt} = -\frac{1}{\rho} \nabla p + \nu \nabla^2 \mathbf{v} \quad (2)$$

where  $\mathbf{v}$  : flow velocity vector  
 $\rho$  : density  
 $p$  : pressure  
 $\nu$  : kinematic viscosity

The vorticity vector is defined as follows;

$$\bar{\zeta} = \text{rot } \mathbf{v} (= \nabla \times \mathbf{v}) \quad (3)$$

The velocity vector  $\mathbf{v}$  can be written with two scalar function  $\psi$  and  $\Phi$ , which satisfy the continuity equation (1) as;

$$\mathbf{v} = \nabla \psi \times \nabla \Phi \quad (4)$$

where  $\Phi$  is chosen for the meridian plane in the case of axisymmetric condition.

The fluid is contained between two concentric spherical shells in which the inner sphere rotates with an arbitrary angular velocity  $\omega$ . In Fig. 1, spherical coordinates system  $(r, \theta, \phi)$  is shown where  $r_1$  is an inner radius and  $r_2$  is an outer radius. Since the flow is axisymmetric, the velocity components can be expressed in terms of the stream function  $\psi(r, \theta; t)$  and the angular velocity function  $\Omega(r, \theta; t)$  where  $\Omega$  is defined according to  $\Phi = \Omega(r, \theta; t)\phi$

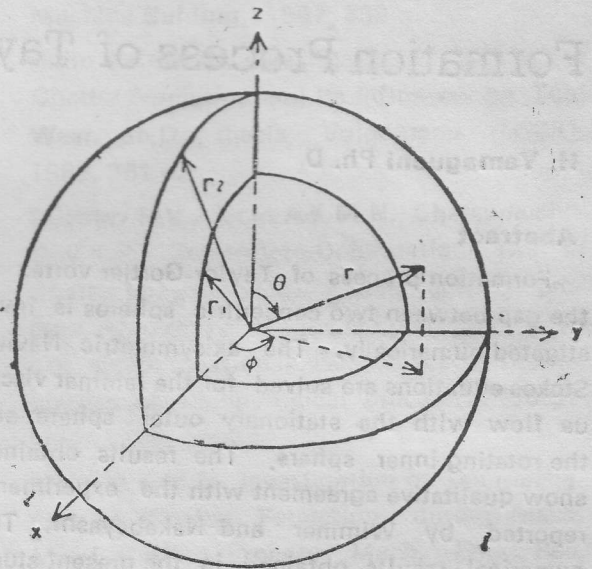


Fig.1 Spherical coordinates system

Therefore, the velocity components are as follows

$$V_r = + \frac{1}{r^2 \sin \theta} \frac{\delta \psi}{\delta \theta} \quad (5)$$

$$V_\theta = - \frac{1}{r \sin \theta} \frac{\delta \psi}{\delta r} \quad (6)$$

$$V_\phi = \frac{\Omega}{r \sin \theta} \quad (7)$$

The momentum equation (2) can be further reduced into the vorticity transport equation as shown below:

$$\frac{\delta \bar{\zeta}}{\delta t} - \nabla \times (\mathbf{v} \times \bar{\zeta}) = -\nu \nabla \times (\nabla \times \bar{\zeta}) \quad (8)$$

finite difference formulae of the equations (16), (17) and (18) is then given by following forms ;

$$F_{i,j}^{n+1} = F_{i,j}^n + F(F_{i,j}^{n+1}, F_{i,j}^n, \Delta t, \Delta R, \Delta \theta, R, \theta, t) \quad (20)$$

$$V_{i,j}^{n+1} = V_{i,j}^n + V(V_{i,j}^{n+1}, V_{i,j}^n, \Delta t, \Delta R, \Delta \theta, R, \theta, t) \quad (21)$$

$$S_{i,j}^{n+1} = S_{i,j}^n + \beta \text{Res} \quad (22)$$

where Res means residual of the finite difference equation and  $\beta$  is a over relaxation factor. It is noted that n is a number of time step and l is a number of iteration.

The vorticity at the walls influences the whole solution in the flow domain. In this study, Jensen's formula of second order of accuracy is used along with Schauf (5).

$$V_{1,j}^{n+1} = \frac{1}{2 \Delta R^2} [7 S_{1,j} - 8 S_{2,j} - S_{3,j}] + 0(\Delta R^2) \quad (23)$$

Accuracy, stability and convergence of the solutions are very much affected by a choice of  $\Delta R$ ,  $\Delta \theta$ ,  $\Delta t$ . In the present study, these parameters are determined from actual runs of computer program in order to meet sufficient accuracy, stability and speed of convergence of the solutions. The parameters used in the numerical calculation are shown in Table. 1.

Table 1. Numerical parameters

Number of division for R	: M=16
Number of division for $\theta$	: N=91
Time step	: $\Delta t=0.111$
Step length for R	: $\Delta R=0.00667$
Step length for $\theta$	: $\Delta \theta=0.0175$
Over relaxation factor	: $\beta=1.4$

The physical parameters used in the calculation are also shown in Table 2. The value of these parameters are mainly quoted from Wimmer's

(2) experiment where Taylor-Görtler vortices are expected to form.

Table 2. Physical parameters

Radius of inner sphere	: $r_1=0.072$	(m)
Radius of outer sphere	: $r_2=0.080$	(m)
Gap ratio	: $\sigma=0.1$	
Kinematic viscosity	: $\nu=1.21 \times 10^4$	(m <sup>2</sup> /s)

The calculations are carried out with a computer HITAC-M280H in Doshisha University computer centre.

## Results and Discussions

The computation was carried out for the steady Reynolds number of 2000. It is noted here that the critical Reynolds number for  $\sigma=0.1$  is approximately 1200 according to Bertles (3). In the present study, therefore, it is assumed  $Re=2000$  for which a steady pair of Taylor-Görtler vortices are expected.

In Fig. 4 the results of the calculation are shown for the stream function, the contour lines of the stream function against time variation, where K indicates the number of time step after the calculation started at  $K=0$  ( $t=0$  sec.). At early stage  $K=1$ , immediately after accelerated from the rest, the flow contained large cell ranging from the pole to equator. This is the secondary flow motion against the basic main flow. The two boundary layers, the inner one at the rotating sphere and the outer one at the stationary sphere, appear in the gap. It is seen from Fig. 4 for  $K=1$  that the inner boundary layer, in which the meridional velocity component is almost parallel to the surface and the flow is directed from the pole to the equator, is thinner than the outer one. This flow mode is also observed for low Reynolds number, which is well below the critical value, in the experimental studies (2) and (3).



The boundary conditions in Fig. 2 are summarized below for (a) to (d).

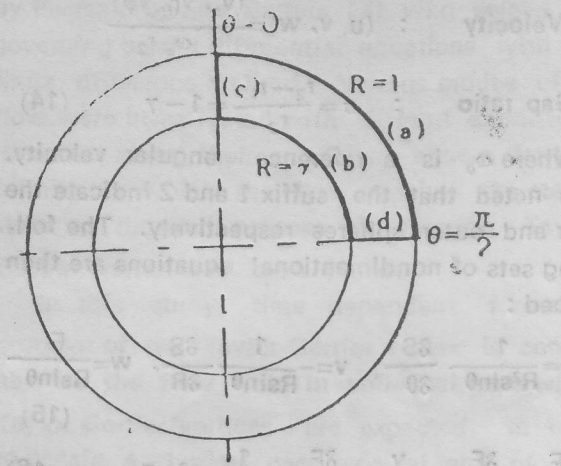


Fig. 2 Boundary conditions

(a)  $R=1, 0 < \theta < \frac{\pi}{2}$

$S=0$

$F=0$

$V = \frac{\delta^2 S}{\delta R^2}, \frac{\delta S}{\delta R} = 0$

(b)  $R=\gamma, 0 < \theta < \frac{\pi}{2}$

$S=0$

$F = \omega_1^* (t) \gamma^2 \sin^2 \theta$

$V = \frac{\delta^2 S}{\delta R^2}, \frac{\delta S}{\delta R} = 0$

(c)  $\theta=0, \gamma \leq R \leq 1$

$S=0$

$F=0$

$V=0$

(d)  $\theta = \frac{\pi}{2}, \gamma \leq R \leq 1$

$S=0$

$\frac{\delta F}{\delta \theta} = 0$

$V=0$

In order to solve the equations (15)-(18) with the boundary conditions given above, the equations are discretized by central differences of second order. The domain of solution consists of equally divided finite difference meshes, as shown in Fig. 3.

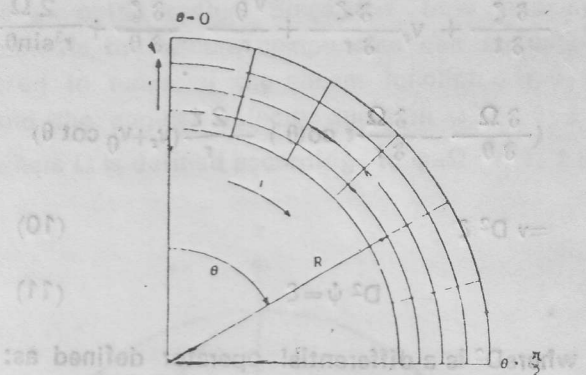


Fig. 3 Finite difference mesh

$R = \gamma + i \Delta R$

$\theta = j \Delta \theta$

$t = n \Delta t$

where

$\Delta R = \frac{\sigma}{M-1}$

$\Delta \theta = \frac{\pi}{2(N-1)}$

Three points approximation formula is used for derivatives appeared in the equations (15-18), in which the truncated error occurred in the calculation is of order  $O(\Delta t^2, \Delta R^2, \Delta \theta^2)$ . For the equations (16) and (17) which include time derivatives, the implicit solution technique with the method used by Peaceman and Rachford (10) is adopted so as to obtain fast convergence and stability of the solutions. On the other hand, for the elliptic type of the equation (18) the successive over relaxation method is used. These methods used in the present study are described elsewhere in the references (6), (7) and (8). The

As time lapses  $K=55$  ( $t=6.11$  sec), on the surface of sphere near the equator  $\theta \approx 80^\circ$ , the meridional velocity decrease in this region. The bou-

ndary layer in this region is thus grown because the meridional mass flux is transported into the layer near the wall. The velocity distributions in

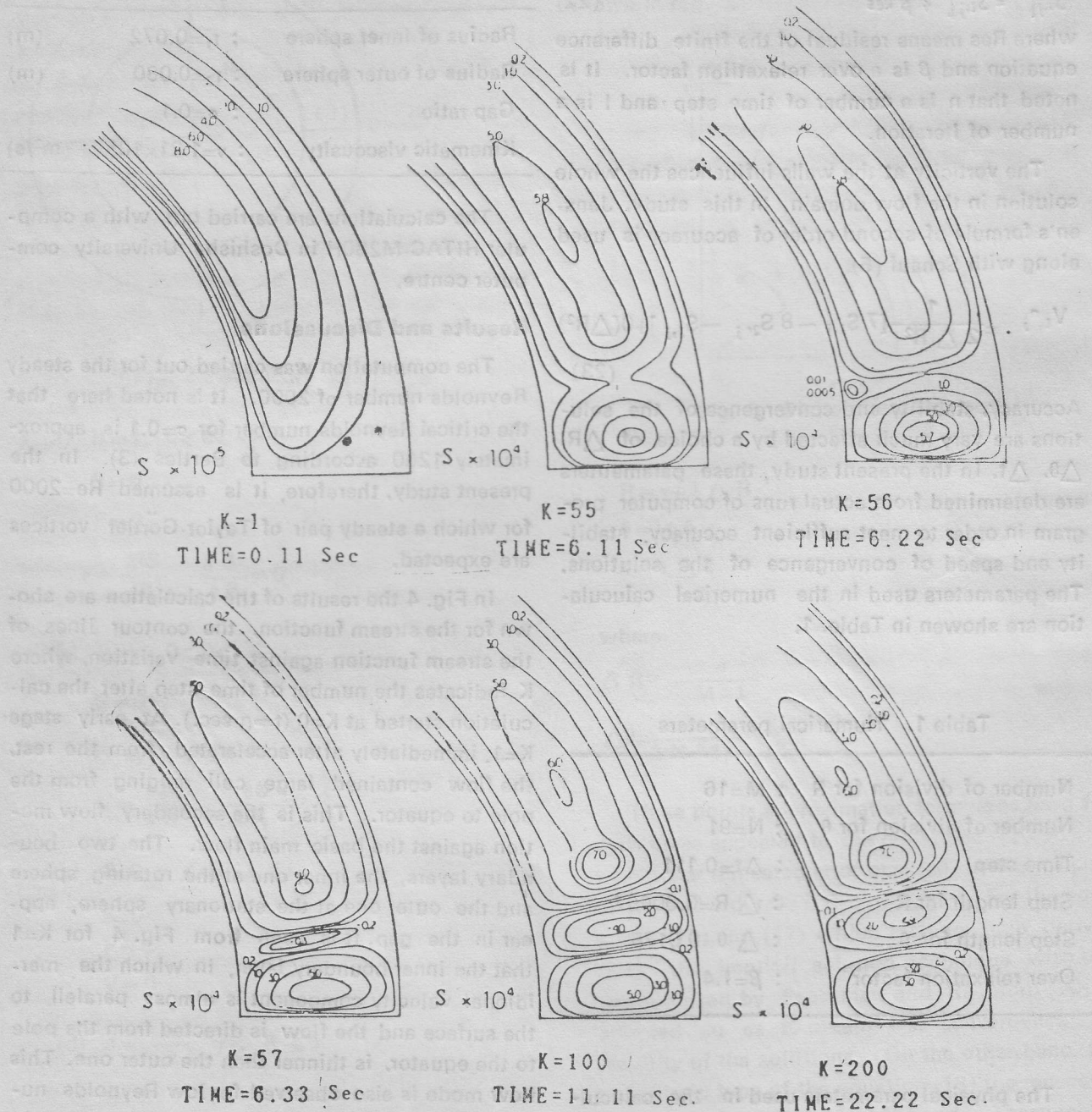


Fig. 4 Stream function contour lines  $Re = 2000$ ,  $\sigma = 0.1$  and  $\Delta t = 0.11$  sec)



this region at  $\theta=81^\circ$  are shown in Fig 5. In Fig. 5 (a) shows the meridional velocity and (b) shows the circumferential velocity as defined below :

$$u' = \frac{u}{F(\gamma, \theta, t) \gamma \sin \theta} \quad (24)$$

$$w' = \frac{w}{F(\gamma, \theta, t) \gamma \sin \theta} \quad (25)$$

It is noted that in Fig. 5,  $u$  has positive value for the direction of increasing  $R$  and  $w$  has positive value for the direction of rotation of the inner sphere. As shown in Fig.5 (a) for  $K=55$

of independent cells occupy the gap space near the equator.

The shape of Taylor-Görtler vortex is almost square whose size is nearly equal to the gap size, although in Fig. 4, some scaling against the radius was done in order to show the vortices clearly. This shape of the vortices are also observed from the experimental studies of Wimmer (2) and Nakabayashi (3).

After formation of Taylor-Görtler vortices in the gap, the configuration of the vortices are almost settled with the passage of time, although

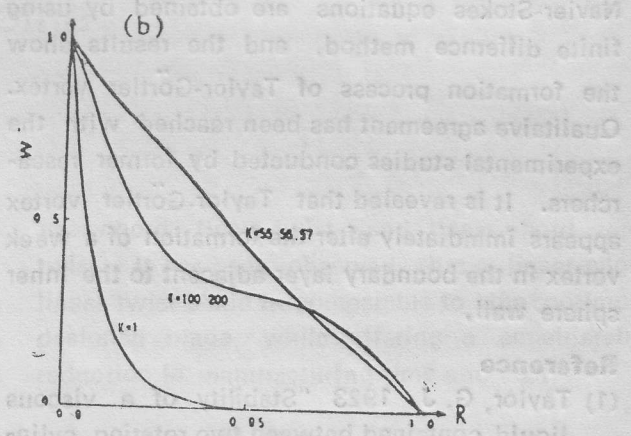
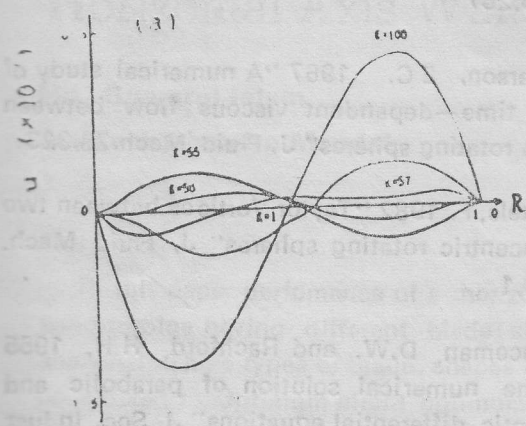


Fig. 5 Velocity distribution ( $\theta=81^\circ$ )

and 56 the decrease of the meridional velocity is obvious. It is thought that in this region at  $K=55$ , the flow condition is similar to that in the flow along a concave curved wall where the boundary layer is unstably stratified. Then on the next instant  $K=56$ , a very weak eddy motion of a small independent vortex appears in the inner boundary layer. This vortex grows and moves toward centre of the gap, causing the separation of the boundary layer. At  $K=57$  as shown in Fig 4, a pair

some movement of the vortices is found. This is shown in Fig. 5 (a) where the velocity  $u$  at  $K=100$  and  $K=200$  are different due to shifting of the cell. This motion might be caused by the Coriolis force physically and from a view point of numerical calculation the solution of the equations are still developing.

In the present study, qualitative agreement has been reached with the results obtained by Wimmer (2) and Nakabayashi (3). However,

in the nature of the flow situation the flow is generally three-dimensional so that the solution must be obtained in a symmetric breaking situation. Particularly, this is important for large gap size. Furthermore, the heat dissipation may be included in the calculation to simulate more general situations. These are out of scope in the present case and further study should be necessary.

### Conclusion

A viscous incompressible fluid contained between two concentric sphere, where the inner one rotates and the outer one is stationary, is investigated. The solutions of the axisymmetric Navier-Stokes equations are obtained by using finite difference method, and the results show the formation process of Taylor-Görtler vortex. Qualitative agreement has been reached with the experimental studies conducted by former researchers. It is revealed that Taylor-Görtler vortex appears immediately after the formation of a weak vortex in the boundary layer adjacent to the inner sphere wall,

### Reference

- (1) Taylor, G. J. 1923 "Stability of a viscous liquid contained between two rotating cylinders" Phil. Trans. A223, 289
- (2) Wimmer, V.I. 1970 "Experiments on a viscous fluid flow between concentric rotating spheres" J. Fluid Mech. 78, 317
- (3) Nakabayashi, K. 1983 "Transition of Taylor Görtler Vortex flow in spherical Couette flow" J. Fluid Mech, 132,209
- (4) Munson, B.R. and Menguturn, M. 1975 "Viscous incompressible flow between concentric rotating spheres. part 3 ; Linear stability and Experiments" J. Fluid Mech. 166,287
- (5) Schrauf, E.C. 1986 "The first instability in spherical Taylor-Couette flow" J. Fluid Mech 166,287
- (6) Pearson, E.C. 1967 "A numerical study of the time—dependent viscous flow between two rotating spheres" J. Fluid Mech.28,323
- (7) Bartels, F. 1982 "Taylor Vortices between two concentric rotating spheres" J, Fluid Mech. 119,1
- (8) Peaceman, D.W. and Rachford, H.H. 1955 "The numerical solution of parabolic and elliptic differential equations" J. Soc. Indust. Appl. Math. Vol. 3 No. 1